

Solvent-Free Synthesis of Zeolites from Solid Raw Materials

Limin Ren,[†] Qinming Wu,[§] Chengguang Yang,[†] Longfeng Zhu,[†] Caijin Li,[†] Pengling Zhang,[†] Haiyan Zhang,[†] Xiangju Meng,^{*,§} and Feng-Shou Xiao^{*,§}

[§]Department of Chemistry, Zhejiang University, Hangzhou 310028, China

[†]Department of Chemistry, Jilin University, Changchun 130012, China

Supporting Information

ABSTRACT: As important industrial materials, microporous zeolites are necessarily synthesized in the presence of solvents such as in hydrothermal, solvothermal, and ionothermal routes. We demonstrate here a simple and generalized solvent-free route for synthesizing various types of zeolites by mixing, grinding, and heating solid raw materials. Compared with conventional hydrothermal route, the avoidance of solvents in the synthesis not only significantly reduces the waste production, but also greatly increases the yield of zeolite products. In addition, the use of starting solid raw materials remarkably enhances the synthesis efficiency and reduces the use of raw materials, energy, and costs.

Zeolites with intricate micropores have been extensively studied for a long time as an important class of industrial porous materials in different areas of chemical industry such as gas adsorption and separation, ion exchange, and shape selective catalysis.^{1–7} Their syntheses normally require the presence of solvents from various methodologies such as hydrothermal, solvothermal, and ionothermal routes.^{8–21} We show here a simple and generalized solvent-free route for synthesizing various zeolites (ZSM-5, silicalite-1, ZSM-39, SOD, MOR, Beta, and FAU) from mixing, grinding, and heating solid raw materials. Chosen as a model case, it is clearly confirmed that silicalite-1 zeolite in the solvent-free synthesis crystallizes from amorphous silicates could be successfully obtained by this convenient approach. This approach should be applicable to the synthesis of a wide variety of zeolitic structures.

Solvent-free synthesis of zeolites with MFI structure was performed by mechanically mixing of solid raw materials of NaSiO₃·9H₂O (SiO₂, 20 wt.%), fumed silica, tetrapropylammonium bromide (TPABr), NH₄Cl, and heteroatom source (The origin of all reagents were provided in the Supporting Information). The heteroatom source could be boehmite, Fe(NO₃)₃·9H₂O, Ga₂O₃, or H₃BO₃, respectively. After grinding for 10–20 min, the mixture was heated in an autoclave at 180 °C for 24–72 h. The samples with various compositions designed as S-M-ZSM-5 (M = Si, Al, Fe, Ga, or B) were obtained,²² as presented in Table S1 and Figure S1. As a typical run for the synthesis of S-Si-ZSM-5 (silicalite-1), 1.315 g of NaSiO₃·9H₂O (SiO₂, 20 wt.%), 0.30–0.36 g of fumed silica, 0.40–0.46 g of NH₄Cl, and 0.24 g of TPABr were added into a mortar one by one and mixed together. After grinding for 10–

20 min, the powder mixture was transferred to an autoclave and sealed. After heating at 180 °C for 24–48 h, the sample was fully crystallized.

Figure S1 shows XRD patterns of S-Si-ZSM-5, S-Al-ZSM-5, S-Fe-ZSM-5, S-B-ZSM-5 and S-Ga-ZSM-5. Notably, they exhibit characteristic peaks associated with MFI structure,²³ indicating the successful synthesis of these zeolites from the solvent-free route. As quite different from hydrothermal synthesis of zeolitic crystals with micrometer sizes,⁸ S-M-ZSM-5 samples synthesized from solvent-free route produce relatively large crystals (Figure 1a–c and Figure S2). This phenomenon would be directly related to the solid phase of reactants in the synthesis, where the solid nutrients or particles aggregated with each other making large polycrystals. ²⁷Al NMR spectrum of S-Al-ZSM-5 with Si/Al ratio at 109 shows a sharp band at 54 ppm (Figure 1e) associated with 4-coordinated Al species.²⁴ UV–visible spectrum (Figure 1f) of the as-synthesized S-Fe-ZSM-5 exhibits a strong band at near 250 nm and a series of weak bands at 372, 410, and 435 nm, in good agreement with those as-prepared Fe-ZSM-5 reported in the literature.²⁵ The strong band at near 250 nm is assigned to Fe³⁺ at isolated tetrahedral framework sites (charge transfer band), and a series of weak bands at higher wavelengths are attributed to d–d transitions of the Fe³⁺ ion in tetrahedral symmetry.²⁵ These results suggest that the solvent-free route is also effective for incorporation of heteroatom into the zeolite framework, which is potentially important for design and preparation of catalytically active zeolites.^{1–7}

Interestingly, the solvent-free route could be also applied to synthesizing hierarchical porous zeolites. After addition of nanosized CaCO₃ (average sizes of 100 nm, Figure S3) as a solid template in the synthesis of S-Si-ZSM-5 (Figure S4) and treatment by acidic solution, the macropores (about 100 nm) are successfully formed in Si-ZSM-5 crystals, confirmed by SEM image (Figure 1d), N₂ sorption (Figure S5), and mercury intrusion results (Figure S6).

Compared with hydrothermal synthesis, the solvent-free route for synthesizing zeolites has the following obvious features: (1) High yields of zeolites. Conventionally, a solvent is necessary for the synthesis of microporous crystalline zeolite, and partial nutrients such as silicates and aluminates still exist in the solvent when the crystallization has been finished, thus, giving a relatively low yield of the products.⁸ This work greatly reduces using the solvents, which can significantly increase the

Received: May 9, 2012

Published: September 6, 2012

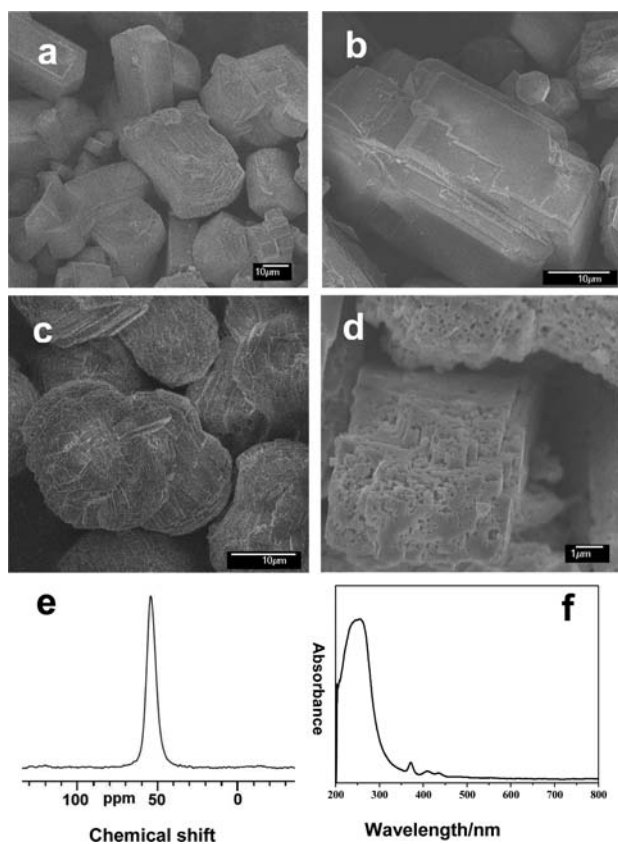


Figure 1. SEM images of (a) S-Si-ZSM-5, (b) S-Al-ZSM-5 with a Si/Al ratio of 109, (c) S-Fe-ZSM-5 with a Si/Fe ratio of 38, (d) S-Si-ZSM-5 synthesized in the presence of CaCO_3 nanocrystals, (e) ^{27}Al NMR spectrum of as-synthesized S-Al-ZSM-5 with a Si/Al ratio of 109, and (f) UV-visible spectrum of as-synthesized S-Fe-ZSM-5 with a Si/Fe ratio of 38.

zeolite yields. For example, the yield for synthesizing S-Si-ZSM-5 zeolite is as high as 93–95%, which is much higher than that (82–86%) of silicalite-1 zeolite from hydrothermal synthesis.⁸ (2) Better utilization of autoclaves. Generally, under hydrothermal conditions, the solvent occupies a large space of autoclaves. However, the “solvent-free” route effectively saves the space of the autoclaves, thus, giving high utilization of the autoclaves. For example, when an autoclave with volume of 13 mL was used to synthesize silicalite-1 zeolite, the solvent-free route gives the product weight of 2.12 g, which is almost 3 times of that (0.75 g) of a typical hydrothermal route.⁸ (3) A significant reduction of pollutants. Normally, the nutrients dissolved in the solvents under hydrothermal conditions are pollutants. In contrast, the solvent-free route nearly completely avoids the use of solvents, maximally reducing the wastes. (4) Saving energy and simplifying synthetic procedures. Usually, hydrothermal synthesis includes preparation of homogeneous starting gels and hydrothermal treatments. In this work, the solvent-free route only involves in grinding and heating the raw solids. (5) A large reduction of reaction pressure. The lack of solvents in the solvent-free route remarkably decreases the reaction pressure.¹⁴ Therefore, the requirement for the high pressure equipment could be avoided in the synthesis. Considering these “green” features, it is believable that the solvent-free route will be of great importance for industrial production of zeolites in the future.

It is worth noting that the solvent-free route is quite distinguishable from “dry gel conversion (DGC)”¹¹ for synthesizing zeolite, where the solvents are necessary for preparation of the homogeneous gels, followed by vaporizing the solvents to obtain the dry gels. Compared with the “DGC” method, this work has very simple procedures, remarkably saving the energy.

To understand the solvent-free route, the crystallization of S-Si-ZSM-5 has been investigated. For a better observation, the mixture was sealed in a closed glass tube for the reaction. Figure 2A shows photographs of the samples crystallized at various times. Clearly, during the crystallization process, the samples are always in a solid phase, confirming the solid reaction. However, the sample volume is reduced remarkably after the treatment, suggesting the condensation of silica species due to the crystallization of S-Si-ZSM-5. Figure 2B–D shows XRD patterns, UV-Raman and ^{29}Si NMR spectra of the samples crystallized at various times, respectively. Before crystallization, the sample exhibits XRD patterns of each raw materials (Figure 2B-a, Figure S7). After the treatment at 180 °C for 2 h, the peaks associated with the raw solids disappear, and a peak related to cubic NaCl phase is observed (interaction between Na_2SiO_3 with NH_4Cl , Figure 2B-b). The disappearance of the XRD peaks is attributed to the spontaneous dispersion of solid salts on the amorphous support due to the increase of entropy (ΔS).^{26–28} At the same time, the bands assigned to TPA^+ species in UV-Raman spectra are greatly reduced after the treatment at 180 °C for 2 h (Figure 2C-a,C-b), which is in good agreement with the high disordering of TPA^+ species with weak Raman signals by the high dispersion of solid salts on the amorphous support.²⁹ As observed from ^{29}Si NMR spectroscopy, the treatment of the sample at 180 °C for 2 h results in a significant condensation of silica species, giving that Q_4 silica species $[\text{Si}(\text{SiO})_4]$ are dominant (Figure 2D-a,D-b). When the crystallization time reaches 10 h, the sample shows weak peaks associated with MFI structure in XRD pattern (Figure 2B-c), an obvious band (374 cm^{-1}) assigned to 5-membered ring of Si-O-Si and sharp bands (e.g., 307 and 1037 cm^{-1}) attributed to TPA^+ in the UV-Raman spectrum (Figure 2C-c) appear, suggesting that a small amount of S-Si-ZSM-5 crystals are formed. With the crystallization time increasing from 10 to 18 h, the intensities of XRD peaks and Raman bands strongly increase (Figure 2B-c to B-e, Figure 2C-c to C-e), indicating the successful transformation from amorphous silica to zeolite crystals. Correspondingly, the degree of silica condensation for the samples is extensively enhanced (Figure 2D-c,D-d). When the crystallization time is over 18 h, there is no obvious change in XRD patterns and UV-Raman spectra of the samples, indicating that the crystallization of S-Si-ZSM-5 zeolite is basically finished (Figure 2B-f, C-f). These results demonstrate that S-Si-ZSM-5 zeolite crystallized through the solid phase transformation, in good agreement with the mechanism on solid-state synthesis of inorganic clusters reported previously.³⁰

It is worth mentioning that we cannot obtain zeolite products from solvent-free route if it is absent of a small amount of water (hydrated form of sodium silicate or hydrated form of silica) in the solid synthesis system. These results suggest that a small amount of water is a critical parameter for the formation of zeolites in the solvent-free route. In addition, the alkalinity of the synthesis system is also important, and the hydrated form of sodium silicate offers a suitable alkalinity for the solvent-free route. A small amount of water and alkalinity of the system are helpful for the synthesis of zeolites by solid interaction, which

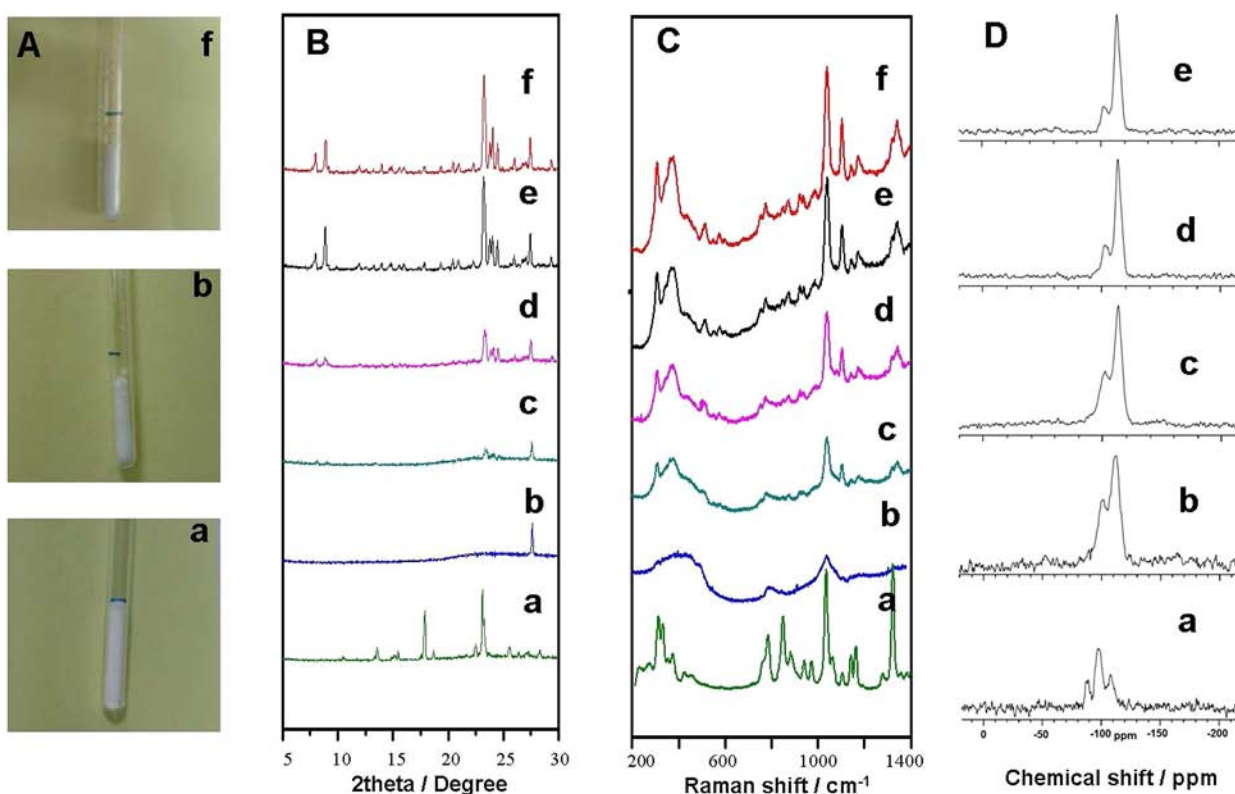


Figure 2. Investigation on S-Si-ZSM-5 crystallization. (A) Photographs, (B) XRD patterns, (C) UV-Raman spectra, (D) ^{29}Si NMR spectra of the samples crystallized at (a) 0, (b) 2, (c) 10, (d) 12, (e) 18, and (f) 24 h for synthesizing S-Si-ZSM-5 zeolite.

might be favorable for facilitating hydrolysis and condensation of Si–O–Si bonds during the synthesis.

Notably, the interaction between the templates of TPA^+ cations with silica species in the solvent-free synthesis is different from those in the hydrothermal synthesis. For example, when heating the starting raw materials for 2 h at $180\text{ }^\circ\text{C}$, the calcined amorphous sample shows typical isotherm for Langmuir adsorption, giving HK pore size distribution at 0.8 nm (Figure S8). These results suggest that the amorphous intermediates already have some microporosity before the formation of the crystalline channels,^{31,32} indicating that TPA^+ cations have been inserted into the amorphous silica by the spontaneous dispersion in solid phase.^{26–28} In contrast, the similar reaction intermediates synthesized in hydrothermal route (hydrothermal treatment at $180\text{ }^\circ\text{C}$ for 0.5 h, as observed in the crystallization curve in Figure S9) does not have any microporosity (Figure S10a). Increasing the crystallization time from 0.5 to 2.5 h (1.0, 2.0, and 2.5 h, respectively), the calcined amorphous samples obtained from hydrothermal route still have no microporosity (Figure S10b–d), suggesting that TPA^+ cations cannot be embedded in amorphous silica in the hydrothermal route. These results indicate the distinguishable mechanism on the crystallization of zeolites between solvent-free and hydrothermal route.

Figure S11 shows thermal analysis (TG-DTA) of S-Si-ZSM-5 zeolite, exhibiting the weight loss of TPA^+ cations at about 10.9 wt.%. After calcination at $550\text{ }^\circ\text{C}$ for 4 h, S-Si-ZSM-5 zeolite shows typical adsorption of MFI zeolite, giving the micropore surface area at $276\text{ m}^2/\text{g}$, t -plot micropore volume at $0.13\text{ cm}^3/\text{g}$, and pore size distribution at 5.3 \AA , in good agreement with those of conventional MFI zeolites synthesized in the presence of organic templates.⁸

Here we have provided the essential results of S-Si-ZSM-5 synthesis for demonstration of our proposed solvent-free synthesis route. We also have successfully synthesized other types of zeolites (ZSM-39, SOD, MOR, Beta, and FAU, Figures S12–S16) using this route. We are currently applying this method using various organic templates and preparing various zeolites by this route. Particularly, the solvent-free synthesis of Beta zeolite combines the advantages of both solid raw materials and organotemplate-free approach,³³ which is potentially important for green synthesis of zeolites.⁷

In summary, a series of zeolite with various framework types have been successfully prepared from solvent-free route through mechanically mixing of solid state raw materials (in the absence of any solvent), followed by heating in the closed vessel. The products exhibited similar chemical and physical properties with the zeolites synthesized from hydrothermal routes. For industrial production of zeolites (requirement of a huge amount of zeolite in the global market), the solvent-free synthesis means significant savings in raw materials, energy, and costs. This methodology opens a new door for synthesizing zeolites and would be potentially important for industrial application of zeolites at a large scale.

■ ASSOCIATED CONTENT

📄 Supporting Information

Synthesis and characterization details. This material is available free of charge via the Internet at <http://pubs.acs.org>.

■ AUTHOR INFORMATION

Corresponding Author

fsxiao@zju.edu.cn

Notes

The authors declare no competing financial interest.

ACKNOWLEDGMENTS

This work was supported by the State Basic Research Project of China (2009CB623507) and the National Natural Science Foundation of China (21273197 and U1162201).

REFERENCES

- (1) Breck, D. W. *Zeolite Molecular Sieves*; Krieger: Malabar, 1984.
- (2) van Bekkum, H.; Flanigen, E. M.; Jacobs, P. A.; Jansen, J. C. *Introduction to Zeolite Science and Practice*; Elsevier: Amsterdam, 2001.
- (3) Barrer, R. M. *Hydrothermal Chemistry of Zeolites*; Academic Press: London, 1982.
- (4) Rabo, J. A. *Zeolite Chemistry and Catalysis*; ACS Monograph; American Chemical Society: Washington, DC, 1976.
- (5) Baerlocher, C.; Meier, W. M.; Olson, D. H. *Atlas of Zeolite Framework Types*; 6th Revised ed.; Elsevier: Amsterdam, 2007.
- (6) Corma, A. *Chem. Rev.* **1995**, *95*, 559.
- (7) Davis, M. E. *Nature* **2002**, *417*, 813.
- (8) Xu, R.; Pang, W.; Yu, J.; Huo, Q.; Chen, J. *Chemistry of Zeolite and Related Porous Materials*; Wiley: Singapore, 2007.
- (9) Bibby, D. M.; Dale, M. P. *Nature* **1985**, *317*, 157.
- (10) (a) Kuperman, A.; Nadimi, S.; Oliver, S.; Ozin, G. A.; Garcés, G. M.; Olken, M. M. *Nature* **1993**, *365*, 239. (b) Huo, Q.; Xu, R. *J. Chem. Soc., Chem. Comm.* **1990**, 783.
- (11) (a) Xu, W.; Dong, J.; Li, J.; Li, J.; Wu, F. *J. Chem. Soc., Chem. Comm.* **1990**, 755. (b) Zhang, L.; Yao, J.; Zeng, C.; Xu, N. *Chem. Commun.* **2003**, 2232. (c) Chen, B.; Huang, Y. *J. Am. Chem. Soc.* **2006**, *128*, 6437.
- (12) Cooper, E. R.; Andrews, C. D.; Wheatley, P. S.; Webb, P. B.; Wormald, P.; Morris, R. E. *Nature* **2004**, *430*, 1012.
- (13) Morris, R. E. *Angew. Chem., Int. Ed.* **2008**, *47*, 442.
- (14) Cai, R.; Liu, Y.; Gu, S.; Yan, Y. *J. Am. Chem. Soc.* **2010**, *132*, 12776.
- (15) Choi, M.; Na, K.; Kim, J.; Sakamoto, Y.; Terasaki, O.; Ryoo, R. *Nature* **2009**, *461*, 246.
- (16) Na, K.; Jo, C.; Kim, J.; Cho, K.; Jung, J.; Seo, Y.; Messinger, R. J.; Chmelka, B. F.; Ryoo, R. *Science* **2011**, *333*, 328.
- (17) Lobo, R. F.; Pan, M.; Chan, I.; Li, H. X.; Medrud, R. C.; Zones, S. I.; Crozier, P. A.; Davis, M. E. *Science* **1993**, *262*, 1543.
- (18) Jiang, J. X.; Jorda, J. L.; Yu, J.; Baumes, L. A.; Mugnaioli, E.; Diaz-Cabanas, M. J.; Kolb, U.; Corma, A. *Science* **2011**, *333*, 1131.
- (19) (a) Fan, W.; Snyder, M. A.; Kumar, S.; Lee, P.-S.; Yoo, W. C.; McCormick, A. V.; Penn, R. L.; Stein, A.; Tsapatsas, A. M. *Nat. Mater.* **2008**, *7*, 984. (b) Yoo, W. C.; Kumar, S.; Penn, R. L.; Tsapatsis, M.; Stein, A. *J. Am. Chem. Soc.* **2009**, *131*, 12377.
- (20) Ng, E. P.; Chateigner, D.; Bein, T.; Valtchev, V.; Mintova, S. *Science* **2012**, *335*, 70.
- (21) Sun, J.; Bonneau, C.; Cantín, A.; Corma, A.; Díaz-Cabañas, M. J.; Moliner, M.; Zhang, D.; Li, M.; Zou, X. *Nature* **2009**, *458*, 1154.
- (22) Ren, L. Ph.D. Thesis, Novel routes for synthesizing of zeolites, Jilin University, 2012.
- (23) Treacy, M. M. J.; Higgins, J. B. *Collection of Simulated XRD Patterns for Zeolites*; 5th Revised ed.; Elsevier: Amsterdam, 2007.
- (24) Triantfillidis, C. S.; Vlessidis, A. G.; Nalbandian, L.; Evmiridis, N. P. *Microporous Mesoporous Mater.* **2001**, *47*, 369.
- (25) (a) Bordiga, S.; Buzzoni, R.; Geobaldo, F.; Lamberti, C.; Giamello, E.; Zecchina, A.; Leofanti, G.; Petrini, G.; Tozzola, G.; Vlaic, G. *J. Catal.* **1996**, *158*, 486. (b) Lin, D. H.; Coudurier, G.; Vedrine, J. C. *Stud. Surf. Sci.* **1989**, *49*, 1431. (c) Hensen, E. J. M.; Zhu, Q.; Janssen, R. A. J.; Magusin, P. C. M. M.; Kooyman, P. J.; van Santen, R. A. *J. Catal.* **2005**, *233*, 123.
- (26) Xie, Y.-C.; Tang, Y.-Q. *Adv. Catal.* **1990**, *37*, 1.
- (27) Lipsch, J. M. J. G.; Schuit, G. C. A. *J. Catal.* **1969**, *15*, 174.
- (28) Xiao, F.-S.; Zheng, S.; Sun, J.; Yu, R.; Qiu, S.; Xu, R. *J. Catal.* **1998**, *176*, 474.
- (29) Dutta, P. K.; Puri, M. *J. Phys. Chem.* **1987**, *91*, 4329.
- (30) Ye, X.; Jia, D.; Yu, J.; Xin, X.; Xue, Z. *Adv. Mater.* **1999**, *11*, 941.
- (31) Fan, F.; Feng, Z.; Sun, K.; Guo, M.; Guo, Q.; Song, Y.; Li, W.; Li, C. *Angew. Chem., Int. Ed.* **2009**, *48*, 8743.
- (32) Corma, A. *Chem. Commun.* **2006**, 3137.
- (33) Xie, B.; Song, J.; Ren, L.; Ji, Y.; Li, J.; Xiao, F. S. *Chem. Mater.* **2008**, *20*, 4533.